PHASE RESETTING EFFECTS FOR ROBUST CYCLES BETWEEN CHAOTIC SETS

PETER ASHWIN, MICHAEL FIELD, ALASTAIR M. RUCKLIDGE, ROB STURMAN

ABSTRACT. In the presence of symmetries or invariant subspaces, attractors in dynamical systems can become very complicated owing to the interaction with the invariant subspaces. This gives rise to a number of new phenomena including that of robust attractors showing chaotic itinerancy. At the simplest level this is an attracting heteroclinic cycle between equilibria, but cycles between more general invariant sets are also possible.

This paper introduces and discusses an instructive example of an ODE where one can observe and analyse robust cycling behaviour. By design, we can show that there is a robust cycle between invariant sets that may be chaotic saddles (whose internal dynamics correspond to a Rössler system), and/or saddle equilibria.

For this model, we distinguish between cycling that include *phase resetting* connections (where there is only one connecting trajectory) and more general *non-phase resetting* cases where there may be an infinite number (even a continuum) of connections. In the non-phase resetting case there is a question of *connection selection*: which connections are observed for typical attracted trajectories? We discuss the instability of this cycling to resonances of Lyapunov exponents and relate this to a conjecture that phase resetting cycles typically lead to stable periodic orbits at instability whereas more general cases may give rise to 'stuck on' cycling.

Finally, we discuss how the presence of positive Lyapunov exponents of the chaotic saddle mean that we need to be very careful in interpreting numerical simulations where the return times become long; this can critically influence the simulation of phase-resetting and connection selection.

Submitted to special issue of *Chaos* on chaotic itinerancy.

Date: September 2003 – *Chaos* **13** 973–981.

Research partially supported by NSF Grant DMS-0071735, and by EPSRC Grants GR/R63530 and GR/N14408.

1. Introduction

One of the main obstructions to a good understanding of the dynamics of high-dimensional coupled systems (such as neural information processing networks) is the relative absence of a clear and useful classification of the attractors that one can typically find; see for example [12, 16]**. For this reason, the recognition that chaotic itinerancy can occur in such systems is a significant step towards a better classification. Similar behaviour, where attractors show robust intermittent behaviour has been seen in models with symmetries or invariant subspaces such as** [13, 8]**; see the review of Krupa** [17]**. Itinerancy in the form of robust heteroclinic cycles has been found in several models for coupled cells; for example** [14, 15, 3]**, and there are related weak notions of attraction such as those considered in** [21, 16, 1] **as well as cycles between chaotic sets** [10]**. This paper examines a specific ODE model for a robust cycle between chaotic and equilibrium saddles that is amenable to analysis. For this model we discuss the qualitative properties of phase resetting connections and the selection of connections.**

There is still much to be understood about the typical form of robust heteroclinic-like attractors. In this paper, we examine a particular feature (phase resetting) that is not present in connections between equilibria but which is common in cycles between more complicated invariant sets. This type of behaviour has been seen in systems of cyclically coupled maps [5, 6] and also in a truncated model of magnetoconvection [7]. However, the analysis of the first system requires the inclusion of singularities in the map while the latter system is too complicated to analyse fully. In this paper we consider a new model ODE on $\mathbf{R}^6$ with symmetry $G = (\mathbf{Z}_2)^3$ where a wide variety of attracting robust cycles are possible. Moreover, the ODE is simple enough to be amenable to analysis.

In Section 2 we describe the ODE which is constructed by coupling a Guckenheimer–Holmes robust heteroclinic cycle [13] with a Rössler system [20] in such a way that

- There are attractors that include cycles between saddle equilibria and saddle chaotic sets.
- The attractors persist under perturbations that preserve the symmetry G.

- The system is well-approximated by a skew product in a neighbourhood of each saddle, but globally is not a skew product system.

This model was developed from a skew product system considered previously in [1]. The skew product structure in this system arose through the Rössler system acting as a forcing system on the Guckenheimer–Holmes system. Our new model breaks the skew product to a more general two-way coupling and allows new and, we believe, more typical behaviour.

In Section 3, we show that the model displays a range of cycling chaotic attractors including cycles between equilibria and chaotic saddles. We also describe how these attractors lose stability. We distinguish between *phase resetting* connections, where there is only one connection between two saddles (or 'nodes') in the cycle, and *non-phase resetting* connections with a possibly infinite number of connections (the latter corresponds to the 'free running' scenario described in [5]). The system has been constructed to show both types of behaviour. We also predict and examine the loss of stability of such robust attracting cycles at resonance bifurcation by using transverse Lyapunov exponents. For the mapping model studied in [5], phase resetting is associated with the bifurcation of an infinity of stable periodic solutions whereas the non-phase resetting results in attractors that are chaotic and approximately follow the cycling. For the cycle studied here, one connection is always non-phase resetting and we observe dynamics exhibiting aspects of both non-phase resetting and phase resetting cycles, but with a complicated detailed structure.

In Section 4 we investigate the classification of more general robust cycling attractors. We highlight the problem of *cycle selection* in non-phase resetting cycles. Specifically, if there are an infinite number of connections, which of them will appear in the ω-limit set for 'typical' initial conditions?

Finally, in Section 5, we mention some problems that arise in the numerical simulation of this cycle. In particular we show how phase resetting may be lost due to numerical inaccuracies and we believe this is an issue that needs to be better understood for simulation of general robust and chaotic itinerant attractors.

2. An ODE model with robust cycling between chaotic saddles

Let S^2 denote the unit sphere in $\mathbf{R}^3$. We will define a coupled system of ODEs on $S^2 \times \mathbf{R}^3$. The uncoupled dynamics will basically be the product of the Guckenheimer–Holmes dynamics with those of the Rössler equation. Throughout, we denote coordinates on $S^2 \times \mathbf{R}^3$ by $(\mathbf{x}, \mathbf{y})$, where $\mathbf{x} = (x_1, x_2, x_3)$ and $\Sigma x_i^2 = 1$.

2.1. The Guckenheimer–Holmes and Rössler systems.

We start by defining a vector field on S^2 that is related to the Guckenheimer–Holmes system. If $Q : \mathbf{R}^3 \to \mathbf{R}^3$ is any smooth function and $\langle \cdot, \cdot \rangle$ the standard inner product, we define a smooth vector field F on S^2 by

$$F(\mathbf{x}) = Q(\mathbf{x}) - \langle Q(\mathbf{x}), \mathbf{x} \rangle \mathbf{x}, \quad \mathbf{x} \in S^2.$$

Note that if Q is radial (a multiple of $\mathbf{x}$) then $F \equiv 0$. We define a parametrized family $F(\mathbf{x}; b, c, d)$ of vector fields on S^2 by taking $Q = (Q_1, Q_2, Q_3)$ where

$$\begin{aligned} Q_1(\mathbf{x}, b, c, d) &= x_1(bx_2^2 + cx_3^2 + dx_2^2x_3^2) \\ Q_2(\mathbf{x}, b, c, d) &= x_2(bx_3^2 + cx_1^2 + dx_3^2x_1^2) \\ Q_3(\mathbf{x}, b, c, d) &= x_3(bx_1^2 + cx_2^2 + dx_1^2x_2^2), \end{aligned}$$

and b, c, d are real parameters.

The equations used in computational simulations are either obtained by constraining $\dot{\mathbf{x}} = F(\mathbf{x})$ to $\mathbf{x} \in S^2$ or by adding radial dynamics that causes S^2 to become attracting. That is, by considering $\dot{\mathbf{x}} = \tilde{F}(\mathbf{x})$ where

$$\tilde{F}(\mathbf{x}) = (1 - |\mathbf{x}|^2)\mathbf{x} + F(\mathbf{x}).$$

The models F and $\tilde{F}$ clearly reduce to the same vector field on S^2, and S^2 is flow-invariant for the dynamics defined by $\tilde{F}$. In Figure 1 we show the dynamics on S^2 for the case $d = 0$ and $b + c$, bc, $b < 0$ (for details and computation, see Field [11, Chapter 6]). Referring to the figure, $\mathbf{e}_1, \mathbf{e}_2, \mathbf{e}_3$ are the positive unit vectors along the x_1, x_2 and x_3-axes respectively and $\mathbf{p} = (1, 1, 1)/\sqrt{3}$. When $bc < 0$, the only zeros of F in the first octant of S^2 are $\mathbf{e}_1, \mathbf{e}_2, \mathbf{e}_3$ and $\mathbf{p}$. The equilibria $\mathbf{e}_1, \mathbf{e}_2, \mathbf{e}_3$ are hyperbolic saddles. If $b + c < 0$ then $\mathbf{p}$ is a source and the saddle connections between $\mathbf{e}_1, \mathbf{e}_2, \mathbf{e}_3$ form an attracting heteroclinic cycle. Since F is

equivariant with respect to the action of G on S^2 defined by $(x_1, x_2, x_3) \mapsto (\pm x_1, \pm x_2, \pm x_3)$, the dynamics in the remaining octants is obtained by repeated reflection in the coordinate planes of the dynamics in the first octant.

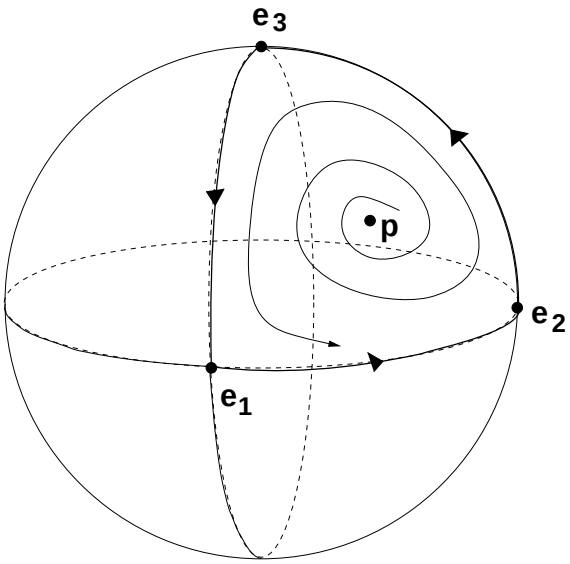

FIGURE 1. Guckenheimer–Holmes dynamics on one octant of the sphere for the case $b + c$, bc, $b < 0$

Remark 2.1. The great circles on S^2 defined by the intersection of S^2 with the coordinate planes are flow-invariant for the dynamics of the vector field F. This invariance is preserved when we couple with the Rössler system and it follows that we shall only need to consider dynamics on the flow-invariant first octant of S^2.

On $\mathbf{R}^3$ the Rössler system $\dot{\mathbf{y}} = G(\mathbf{y})$ (with specific parameter choices) is defined by

$$\begin{aligned} G_1(\mathbf{y}) &= -y_2 - y_3 \\ G_2(\mathbf{y}) &= y_1 + 0.2y_2 \\ G_3(\mathbf{y}) &= 0.2 + y_3(y_1 - 5.7) \end{aligned}$$

and it is well known (see for example [20]) that solutions of this system with initial conditions close enough to the origin are observed to converge to a compact chaotic attractor $\mathcal{A}$. In addition to $\mathcal{A}$, the system has equilibria at

$$\mathbf{y}^A \approx (0.007, -0.035, 0.035), \quad \text{and} \quad \mathbf{y}^B \approx (-5.71, 28.54, -28.54).$$

Both equilibria are hyperbolic saddles: $\mathbf{y}^A$ has a 1-dimensional stable manifold and a 2-dimensional unstable manifold with expanding complex eigenvalues; $\mathbf{y}^B$ has 1-dimensional stable and 2-dimensional unstable manifolds with real eigenvalues. However, the second equilibrium will not be of particular interest for the parameter values considered in this paper.

2.2. **Definition of the coupled system.** We define a smooth map $\mu : S^2 \to \mathbf{R}$ by

$$\mu(\mathbf{x}) = \frac{\tanh(4(2{x_1}^2 - 1)) + \tanh(4)}{2\tanh(4)}.$$

The function μ is chosen to that $\mu(0) = 0$, μ is even in x_1, and $\mu(\pm 1) = 1$. Moreover, μ increases monotonically with the greatest rate of change occurring near the circles $x_1 = \pm\frac{1}{2}$ on the unit sphere.

For $\epsilon > 0$, let Δ_ϵ denote the diagonal matrix $\mathrm{diag}(\epsilon, 2\epsilon, 3\epsilon)$ and pick a fixed vector $\mathbf{y}^F = (y_1^F, y_2^F, y_3^F) \in \mathbf{R}^3$. The dynamics of the $\mathbf{y}$-variables will be coupled to the $\mathbf{x}$-variables by the $\mathbf{x}$-dependent term $-\mu(\mathbf{x})\Delta_\epsilon(\mathbf{y} - \mathbf{y}^F)$. We also couple the $\mathbf{x}$ dynamics to the $\mathbf{y}$ dynamics by making the coefficients b and c functions of $\mathbf{y}$.

We define our coupled system of ODEs on $S^2 \times \mathbf{R}^3$ by

$$\begin{aligned} \dot{\mathbf{x}} &= F(\mathbf{x}; b(\mathbf{y}), c(\mathbf{y}), d), \\ \dot{\mathbf{y}} &= (1 - \mu(\mathbf{x}))G(\mathbf{y}) - \mu(\mathbf{x})\Delta_\epsilon(\mathbf{y} - \mathbf{y}^F), \end{aligned} \tag{1}$$

where

$$b(\mathbf{y}) = b_0 + b_1 \sin(y_1), \quad c(\mathbf{y}) = c_0 + c_1 \sin(y_3).$$

Observe that when $\mu = 0$ (and $x_1 = 0$, $x_2^2 + x_3^2 = 1$), the $\mathbf{y}$ dynamics are identical to the Rössler equations, whereas for $\mu = 1$ ($x_1 = \pm 1$, $x_2 = x_3 = 0$), $\mathbf{y}$ has an attracting fixed point at $\mathbf{y}^F$.

The group $(\mathbf{Z}_2)^3$ of reflections on S^2 extends to the action on $S^2 \times \mathbf{R}^3$ defined by

$$(x_1, x_2, x_3, y_1, y_2, y_3) \mapsto (\pm x_1, \pm x_2, \pm x_3, y_1, y_2, y_3)$$

Since μ is clearly $(\mathbf{Z}_2)^3$-invariant, it follows that for any choice of parameters, the system (1) is symmetric with respect to $(\mathbf{Z}_2)^3$.

Remark 2.2. The Guckenheimer–Holmes [13] model is also symmetric with respect to the $\mathbf{Z}_3$-action defined by $(x_1, x_2, x_3) \mapsto (x_2, x_3, x_1)$. However, μ is not $\mathbf{Z}_3$-invariant and so (1) is

Name	Intersection with $\mathbf{F}$	Subspace	Dim
$\pm P_1$	P_1	$\{\pm\mathbf{e}_1\} \times \mathbf{R}^3$	3
$\pm P_2$	P_2	$\{\pm\mathbf{e}_2\} \times \mathbf{R}^3$	3
$\pm P_3$	P_3	$\{\pm\mathbf{e}_3\} \times \mathbf{R}^3$	3
M	$\mathbf{p}$	$\{\mathbf{p}\} \times \mathbf{R}^3$	3
N_{12}	E_{12}	$S_{12} \times \mathbf{R}^3$	4
N_{23}	E_{23}	$S_{23} \times \mathbf{R}^3$	4
N_{13}	E_{13}	$S_{13} \times \mathbf{R}^3$	4

TABLE 1. With the exception of M, all these subspaces of $S^2 \times \mathbf{R}^3$ (or $\mathbf{F}$) are invariant for any $(\mathbf{Z}_2)^3$-symmetric flow on $S^2 \times \mathbf{R}^3$. The second column gives the notation we use for the intersection of this space with $\mathbf{F}$.

not $\mathbf{Z}_3$-symmetric. Indeed, we have deliberately broken the $\mathbf{Z}_3$ symmetry to ensure that we can obtain cycles between saddles with different dynamics. However, it is easy to verify that the subspace $\{\mathbf{p}\} \times \mathbf{R}^3$ *is* flow-invariant for the system (1). Solutions lying on this subspace can be regarded as *synchronized* solutions. These solutions will not play a major role for us in this paper.

For $i < j \in \{1, 2, 3\}$, let S_{ij} denote the great circle of S^2 defined as the intersection of the $x_i x_j$-coordinate plane with S^2. Each S_{ij} is flow-invariant for every $(\mathbf{Z}_2)^3$ symmetric flow on S^2. The pairwise intersections of all the circles S_{ij} define the points $\pm\mathbf{e}_k$, $k = 1, 2, 3$, which must be flow-invariant, and therefore equilibria, for every $(\mathbf{Z}_2)^3$ symmetric flow on S^2. Let $\mathbf{O} = \{\mathbf{x} \ : \ x_1 \geq 0, \ x_2 \geq 0 \ \text{ and } x_3 \geq 0\}$ denote the positive octant of S^2. Set

$$\mathbf{F} = \mathbf{O} \times \mathbf{R}^3 \subset S^2 \times \mathbf{R}^3,$$

and let E_{ij} denote the flow-invariant subsets of $S^2 \times \mathbf{R}^3$ defined by the intersection of $S_{ij} \times \mathbf{R}^3$ with $\mathbf{F}$.

In Table 1 we list the subspaces of $S^2 \times \mathbf{R}^3$ and $\mathbf{F}$ that are flow-invariant for (1). These are depicted schematically in Figure 2.

It follows from Table 1 that $\partial\mathbf{F} = \cup_{i,j} E_{ij}$ is flow-invariant and so $\mathbf{F}$ is a flow-invariant subspace of $S^2 \times \mathbf{R}^3$. Moreover, just as for the Guckenheimer–Holmes system, once we can

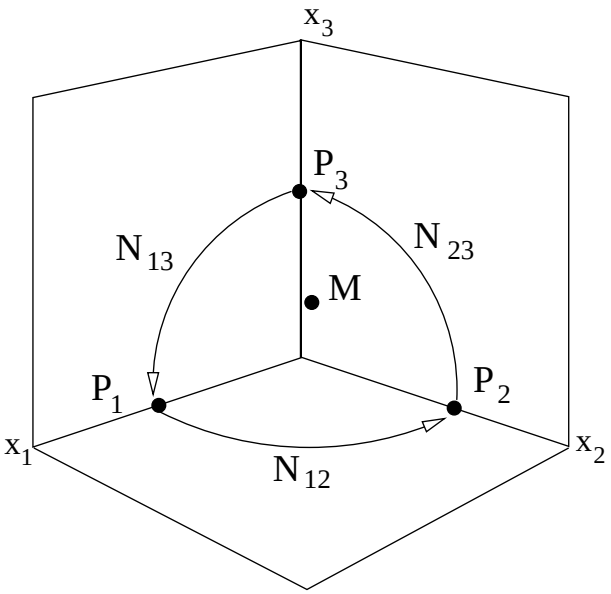

FIGURE 2. A schematic representation of the invariant subspaces for the system (1) projected onto the x_i-coordinates. There can be robust connections between invariant sets in the P_i with connections in the illustrated invariant subspaces N_{ij}.

describe the flow on $\mathbf{F}$ we can obtain the rest of the flow on $S^2 \times \mathbf{R}^3$ by applying symmetry transformations ($\mathbf{F}$ is a *fundamental domain* for the action of $(\mathbf{Z}_2)^3$ on $S^2 \times \mathbf{R}^3$). Henceforth in this paper we will restrict attention to the flow of (1) on $\mathbf{F}$.

The dynamics of the $\mathbf{y}$ variables in the system can be characterized as follows: On the subspace E_{23} of $\mathbf{F}$ defined by $x_1 = 0$, the dynamics are those of the Rössler equation and so trajectories starting close enough to the origin will typically be asymptotic to a Rössler attractor $\mathcal{A}$. On the other hand, when $x_1 = 1$ (and $x_2 = x_3 = 0$), then the dynamics on P_1 will be asymptotic to the globally attracting fixed point $\mathbf{y}^F$ with eigenvalues $-\epsilon, -2\epsilon, -3\epsilon$. Roughly speaking, for initial conditions $\mathbf{x}_0$ between these states, trajectories projected into $\mathbf{R}^3$ – $\mathbf{y}$-space – vary between these extreme states. For future reference, we define

$$\mathcal{A}_j = \{\mathbf{e}_j\} \times \mathcal{A} \subset P_j$$

for $j = 2, 3$, The sets $\mathcal{A}_j$ are Rössler attractors for the flow of (1) restricted to P_j, $j = 2, 3$.

2.3. **Equilibria for the coupled system.** The system (1) has five hyperbolic equilibria in the flow-invariant set $P_1 \cup P_2 \cup P_3$. We shall be interested in three of these equilibria:

$$\mathbf{q}_1 = (\mathbf{e}_1, \mathbf{y}^F),\ \mathbf{q}_2 = (\mathbf{e}_2, \mathbf{y}^A),\ \text{ and }\ \mathbf{q}_3 = (\mathbf{e}_3, \mathbf{y}^A).$$

(The other two equilibria are $(\mathbf{e}_2, \mathbf{y}^B)$ and $(\mathbf{e}_3, \mathbf{y}^B)$.)

The issue of whether or not there exist any other equilibria in $\partial\mathbf{F}$ for (1) is trickier and we sketch only some partial results. Let e_{ij} denote the edge $S_{ij} \cap \mathbf{O}$, $i < j \in \{1, 2, 3\}$. If $(\mathbf{x}, \mathbf{y}) \in \partial\mathbf{F}$ is a hyperbolic equilibrium with $\mathbf{x}$ interior to the edge e_{ij}, then we must have

$$(b_0 + b_1 \sin y_1)(c_0 + c_1 \sin y_3) > 0. \tag{2}$$

If we replace $\mu(\mathbf{x})$ in (1) by the new variable $a \in (0, 1)$, we find two equilibrium points $\mathbf{u}(a), \mathbf{v}(a)$ for $\mathbf{y}$. These can determine equilibrium points of (1) only if (2) is satisfied. For example, if $|b_0| > |b_1|, |c_0| > |c_1|$ and $b_0 c_0 < 0$ then we can never satisfy (2) and so in this case there must be exactly five equilibrium points in $\partial\mathbf{F}$.

If U is an open isolating neighborhood of the Rössler attractor $\mathcal{A} \subset \mathbf{R}^3$ and $b(\mathbf{y})c(\mathbf{y}) < 0$, all $\mathbf{y} \in U$, then there will be no equilibria of (1) in $e_{23} \times U \subset E_{23}$. This implies that all trajectories in interior(E_{23}) with initial conditions close enough to $\mathcal{A}_2 \subset P_2$ will be forward asymptotic to $\mathcal{A}_3 \subset P_3$. Rather than this strong assumption, we will instead choose parameter values (see §3) such that the *ergodic average* of $b(\mathbf{y})c(\mathbf{y})$ over $\mathcal{A}$ is negative.

Matters are more difficult when we study the dynamics on interior(E_{12}) and interior(E_{31}). One way of proceeding is to replace the smooth function μ with a discontinuous threshold function, say

$$\begin{aligned} \bar{\mu}(\mathbf{x}) &= 0,\ |x_1| < \frac{1}{2}, \\ &= 1,\ |x_1| \geq \frac{1}{2}. \end{aligned}$$

The advantage of using a function of this form is that it now becomes relatively easy to obtain precise analytical estimates (see [11]). The disadvantage is that it becomes much harder to estimate errors in numerical investigations. In any case, if we assume that

(1) $b(\mathbf{y})c(\mathbf{y}) < 0$, all $\mathbf{y} \in U$, where U is an isolating neighborhood of $\mathcal{A}$ and
(2) $\mathbf{y}^F \in U$

then it is possible to verify that in this case there are no new equilibria in $\partial\mathcal{O} \times U$ and that every trajectory starting in $\partial\mathcal{O} \times U$ stays in $\partial\mathcal{O} \times U$ and is forward asymptotic to either $\mathbf{y}^F$ or one of $\mathcal{A}_2$, $\mathcal{A}_3$. This result continues to hold if we approximate $\bar{\mu}$ by a smooth function equal to $\bar{\mu}$ away from a small neighborhood of $|x_1| = 1/2$.

2.4. **Stabilities of the equilibria forced by symmetry.** Given any $\mathbf{y} \in \mathbf{R}^3$, we define

$$\eta(\mathbf{y}) = (b_0 + b_1 \sin y_1)(c_0 + c_1 \sin y_3) = b(\mathbf{y})c(\mathbf{y}).$$

Since we are interested in cycles we consider only the case in which $\eta(\mathbf{y}^F) < 0$, $\eta(\mathbf{y}^A) < 0$. This guarantees that each of these equilibria has one expanding and one contracting eigendirection on S^2. Note that though this is not a sufficient condition for the existence of a cycle, as we have no information about $\eta(\mathbf{y})$ for general $\mathbf{y}$, it does enable us to compute the dimensions of stable and unstable manifolds of the equilibria. Furthermore we restrict to the case $b(\mathbf{y}^F) < 0$, $b(\mathbf{y}^A) < 0$, so that the orientation of a cycle has to be $\mathbf{e}_1 \to \mathbf{e}_2 \to \mathbf{e}_3 \to \mathbf{e}_1$. Since $\mathbf{y}^A$ is a fixed point of the Rössler system, and since $\mathbf{y}^F$ is an $\mathbf{x}$-independent equilibrium of $(\mathbf{y}-\mathbf{y}^F)$, the subspaces $(\mathbf{e}_1, \mathbf{y}^F)$, $(\mathbf{e}_2, \mathbf{y}^A)$, $(\mathbf{e}_3, \mathbf{y}^A)$ and $e_{23} \times \{\mathbf{y}^A\}$ are invariant. If $\mathbf{y}^F = \mathbf{y}^A$, all the subspaces $(\mathbf{e}_i, \mathbf{y}^F)$ and $e_{ij} \times \{\mathbf{y}^F\}$ are invariant.

If we regard S^2 as embedded in $\mathbf{R}^3$ and compute the Jacobian in $\mathbf{R}^3 \times \mathbf{R}^3$ we find for example that

$$J(\mathbf{q}_2) = \begin{pmatrix} b_0 + b_1 \sin y_1^A & 0 & 0 & 0 \\ 0 & 0 & 0 & 0 \\ 0 & 0 & c_0 + c_1 \sin y_3^A & 0 \\ 0 & 0 & 0 & E(\mathbf{y}^A) \end{pmatrix}$$

where $E(\mathbf{y})$ is the Jacobian of the Rössler equation at $\mathbf{y}$. The row of zeros follows since S^2 is flow-invariant for (1) and the (normal or radial) $\partial/\partial x_j$ derivative is zero at $\mathbf{e}_2$. (For $\tilde{F}$ we have a -2 eigenvalue since S^2 is flow-invariant and globally attracting for (1). The radial direction is disregarded in the following discussion of dimensions.) The block diagonal structure of the matrix gives the dimensions of stable and unstable manifolds of the equilibria directly. Hence the eigenvalues of the Jacobian of (1) at $\mathbf{q}_2$ are $b_0 + b_1 \sin y_1^A$, $c_0 + c_1 \sin y_3^A$ together with three eigenvalues for Rössler equations at $\mathbf{y}^A$ (recall that $E(\mathbf{y}^A)$ has one negative eigenvalue

and two eigenvalues with positive real part). Thus the points $\mathbf{q}_j$, $j = 2, 3$, have a three-dimensional unstable manifold consisting of the two unstable directions leading to $\mathcal{A}_j$ and the unstable direction normal to P_j. Evaluating the Jacobian at the point $\mathbf{q}_1$ similarly gives a diagonal matrix with diagonal entries $b_0 + b_1 \sin y_1^F$, 0, $c_0 + c_1 \sin y_3^F$, $-\epsilon$, -2ϵ, -3ϵ. Hence the point $\mathbf{q}_1$ has a one-dimensional unstable manifold.

In the following we will assume that $\mathbf{y}^F$ is close to $\mathbf{y}^A$. It is important to note that if $\mathbf{y}^F = \mathbf{y}^A$, then the unstable manifold of $\mathbf{q}_1$ cannot be transverse to the stable manifold of $\mathbf{q}_2$. Indeed, if $\mathbf{y}^F = \mathbf{y}^A$, then the unstable manifold of $\mathbf{q}_1$ (in $\mathbf{F}$) is $e_{12} \times \{\mathbf{y}^F\}$ (less the point $\mathbf{q}_2 = (\mathbf{e}_2, b\mathbf{y}^F)$) and is therefore *contained* in the stable manifold of $\mathbf{q}_2$. When $\mathbf{y}^F \neq \mathbf{y}^A$, the unstable manifold of $\mathbf{q}_1$ does not intersect the stable manifold of $\mathbf{q}_2$.

We sum up our computations and observations in the next lemma and Figure 3. The connections between sets are verified numerically in the next section.

Lemma 2.3. *There is a non-empty open set of parameters b_0, b_1, c_0, c_1, d, ϵ and $\mathbf{y}^F$ such that*

$$\dim(W^u(\mathbf{q}_1)) = 1, \quad \textit{and } \dim(W^u(\mathbf{q}_2)) = \dim(W^u(\mathbf{q}_3)) = 3.$$

If we assume that

$$W^u(\mathcal{A}_2) \subset W^s(\mathcal{A}_3), \ W^u(\mathcal{A}_3) \subset W^s(\mathbf{q}_1),$$

and

$$W^u(\mathbf{q}_1) \subset W^s(\mathbf{q}_2 \cup \mathcal{A}_2), \ W^u(\mathbf{q}_2) \subset W^s(\mathcal{A}_2 \cup \mathbf{q}_3 \cup \mathcal{A}_3), \ W^u(\mathbf{q}_3) \subset W^s(\mathcal{A}_3 \cup \mathbf{q}_1).$$

Then

$$W^u(\mathbf{q}_1) \subset \begin{cases} W^s(\mathbf{q}_2) & \textit{for } \mathbf{y}^F = \mathbf{y}^A \\ W^s(\mathcal{A}_2) & \textit{for } \mathbf{y}^F \neq \mathbf{y}^A \end{cases}$$

and the system has heteroclinic networks as illustrated in Figure 3.

Our system has a total of nine real parameters: b_0, b_1, c_0, c_1, d, ϵ, and $\mathbf{y}^F$. The cycles shown in Figure 3 are only robust for the case $\mathbf{y}^F \neq \mathbf{y}^A$; and then they will be present for a non-empty open set of parameter values. In the next section we examine the stability of the cycles.

Referring to the figure, we remark that P_1 contains the equilibrium point $\mathbf{q}_1$ which is attracting within P_1. The invariant subspaces P_2 and P_3 contain the saddle points $\mathbf{q}_j$,

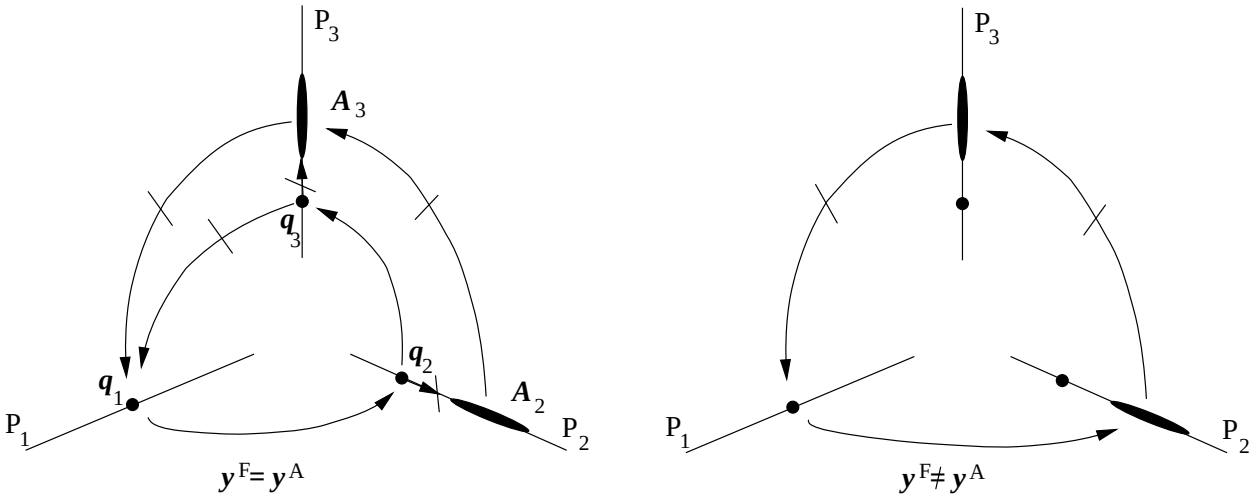

FIGURE 3. The dynamics on $\partial\mathbf{F}$ for $\mathbf{y}^F = \mathbf{y}^A$, and the more general case $\mathbf{y}^F$ not equal but close to $\mathbf{y}^A$. The connections that are crossed consist of an infinite number of connections, while those that are not crossed are phase resetting. For $\mathbf{y}^A = \mathbf{y}^F$ the connection in E_{12} occurs between equilibria, otherwise it is from equilibrium to chaotic saddle.

$j = 2, 3$, as well as copies of the Rössler attractor $\mathcal{A}$. Stabilities of the saddle points in $\partial\mathbf{F}$ are as indicated in Figure 3. The saddle points $\mathbf{q}_j$, $j = 2, 3$ have invariant manifolds contained within $\partial\mathbf{F}$ and $\dim W^u(\mathbf{q}_j) = 3$, $\dim W^s(\mathbf{q}_j) = 2$ in both cases. Since $\mu \equiv 0$ on E_{23}, it follows easily from the explicit equations that $W^u(\mathbf{q}_2)$ intersects $W^s(\mathbf{q}_3)$ transversally along the connection $e_{23} \times \{\mathbf{y}^A\}$. Generically, we expect that $W^u(\mathbf{q}_2)$ meets $W^s(\mathbf{q}_3)$ transversally within all of E_{23} in which case there exist finitely many connections from $\mathbf{q}_2$ to $\mathbf{q}_3$. Although in principle therefore there can exist more than one connection from $\mathbf{q}_2$ to $\mathbf{q}_3$, we mark the connection $\mathbf{q}_2 \to \mathbf{q}_3$ as phase resetting.

3. Attractors involving cycling for the model

Robust homoclinic cycles between invariant sets can gain or lose stability at a *resonance bifurcation* – that is, for parameter values at which the expanding and contracting eigenvalues become equal in magnitude [9]. A similar mechanism, using Lyapunov exponents in place of eigenvalues, can cause cycles between chaotic saddles to gain and lose stability; see for example [1, 7]. The presence in (1) of invariant subspaces greatly simplifies the calculation of the normal Lyapunov exponents. The cycle in question is between 3 invariant subspaces

– one containing an equilibrium, and two containing chaotic saddles, respectively $\mathbf{q}_1$, $\mathcal{A}_2$ and $\mathcal{A}_3$. To calculate the normal Lyapunov exponents of the cycle we multiply together the normal Lyapunov exponents of the constituent parts of the cycle. As earlier, the block diagonal structure of the Jacobian makes it very simple to calculate these exponents. In particular, the contracting and expanding normal Lyapunov exponents at $\mathbf{q}_1$, which we call $\lambda_c^{(\mathbf{q}_1)}$ and $\lambda_e^{(\mathbf{q}_1)}$ respectively, are given by $\lambda_c^{(\mathbf{q}_1)} = b_0 + b_1 \sin y_1^F$ and $\lambda_e^{(\mathbf{q}_1)} = c_0 + c_1 \sin y_3^F$. The normal exponents at $\mathcal{A}_2$ and $\mathcal{A}_3$ can also be found (see [1]) by averaging the derivatives. Hence for an ergodic invariant measure supported on $\mathcal{A}_2$ the transverse Lyapunov exponents are

$$\lambda_c^{(\mathcal{A}_2)}(\mu) = \int_{\mathcal{A}_2} b(u,v,w) d\mu(u,v,w)$$
$$\lambda_e^{(\mathcal{A}_2)}(\mu) = \int_{\mathcal{A}_2} c(u,v,w) d\mu(u,v,w)$$

and similarly for $\mathcal{A}_3$. These can be approximated as in [1] to give

$$(\lambda_c^{(\mathcal{A}_2)}, \lambda_e^{(\mathcal{A}_2)}) = (\lambda_c^{(\mathcal{A}_3)}, \lambda_e^{(\mathcal{A}_3)}) = (b_0 - 0.05360 b_1, c_0 + 0.11629 c_1).$$

If we define

$$\rho := \left| \frac{\lambda_c^{(\mathbf{q}_1)} \lambda_c^{(\mathcal{A}_2)} \lambda_c^{(\mathcal{A}_3)}}{\lambda_e^{(\mathbf{q}_1)} \lambda_e^{(\mathcal{A}_2)} \lambda_e^{(\mathcal{A}_3)}} \right|,$$

then we expect the cycle to be asymptotically stable for $\rho > 1$ (since in this case the normal contraction onto the cycle dominates over the expansion), and unstable for $\rho < 1$. The resonance of Lyapunov exponents occurs at $\rho = 1$. We use c_0 as a control parameter to govern the stability of the cycle. Fixing b_0, b_1, c_1, the resonance condition gives a cubic equation for c_0^* (the value of c_0 at resonance). In all of the following numerics we set $b_0 = -0.1$, $b_1 = c_1 = 0.5$, so that the resonance condition becomes

$$644.604(c_0^* + 0.01756)(c_0^* + 0.05814)^2 = 1,$$

which gives $c_0^* = 0.07285$. Note that for these parameters, we have $\eta(\mathbf{y}) < 0$ for ergodic trajectories within $\mathcal{A}_2$. We also fix throughout the following $d = -0.1$, $\epsilon = 1$.

It is natural to ask what type of attractors are created when cycling chaos loses stability (or equivalently, to describe the mechanisms involved in the creation of cycling chaos). These

matters have been addressed in [5, 6, 7], with particular reference to the difference between phase resetting effects. A phase resetting connection occurs when there is only one trajectory between two invariant sets. In contrast, for non-phase resetting connections, an infinite number of different connecting trajectories may be present.

These computations assume that we are in the case $\mathbf{y}^F \neq \mathbf{y}^A$. Observe moreover that the connection from $\mathcal{A}_2$ to $\mathcal{A}_3$ is always non-phase resetting. In the other case $\mathbf{y}^A = \mathbf{y}^F$ the stability of the cycle may also depend on eigenvalues at $\mathbf{q}_2$ and $\mathbf{q}_3$. Previous papers [5, 6, 7] have conjectured that phase resetting connections usually give rise to stable periodic orbits whose periods accumulate at a resonance, whereas non-phase resetting connections may not. For the cycles discussed in this paper where some connections may be phase resetting and others are not, we find trajectories that are representative of both types of behaviour, but whose detailed structure is a complicated combination.

3.1. **Some numerical results.** Accurate simulation of (1) requires some care. As an attracting cycle approaches the invariant subspaces, some of the $\mathbf{x}$ variables get extremely close to zero, while the $\mathbf{y}$ variables remain $O(1)$. These hugely differing scales result in the potential for phenomena which are purely numerical artefacts and some problems caused by this are addressed in more detail in Section 5. Figure 4 shows convergence towards a cycling chaotic attractor for $c_0 = 0.07$, and $\mathbf{y}^F = (0.01, 1, 0.01)$. The same trajectory is shown in Figure 5 in logarithmic x coordinates. For these parameter values, the saddle point $\mathbf{q}_1$ has one positive eigenvalue for the Jacobian and so the connection from $\mathbf{q}_1 \to \mathcal{A}_2$ is phase resetting. The successive approaches to the connections are shown in Figure 6. Plot (a) shows that the connection $\mathbf{q}_1 \to \mathcal{A}_2$ is phase resetting while the connection $\mathcal{A}_2 \to \mathcal{A}_3$ shown in (b) is non phase resetting (see also Figure 9). In Figure 6 the connection $\mathbf{q}_1 \to \mathbf{q}_2$ is shown in the case $c_0 = 0.07$ and $\mathbf{y}^F = \mathbf{y}^A$. Numerical errors in the specification of $\mathbf{y}^F$ however mean that the connection from $\mathbf{q}_1$ to $\mathbf{q}_2$ is not exact and in fact we see the same effect as a phase resetting connection (a), just with a long time of residence near $\mathbf{q}_2$ (shown by $y_2 = 0$ in this plot); we expect great sensitivity to noise in this case.

Each time round the cycle the dynamics get closer to the invariant subspaces E_{ij}, and this is reflected in the approximately geometric increase of the length T_n of the nth epoch (see for example [6]). Also plotted is y_2, depicting the change in behaviour of the $\mathbf{y}$ variables, as

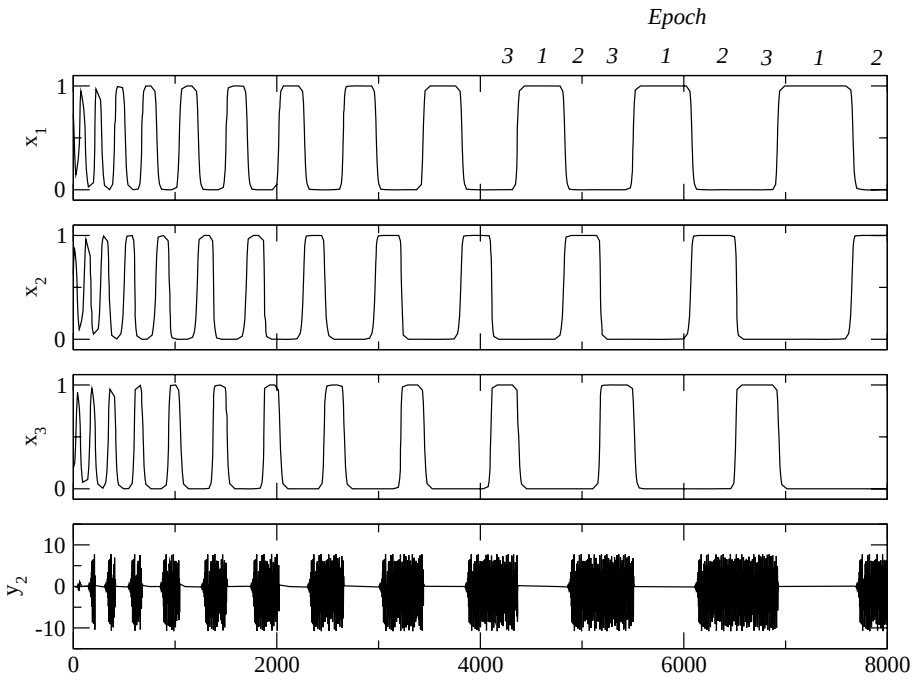

FIGURE 4. A trajectory approaching a cycling chaotic attractor for $b_0 = -0.1$, $b_1 = 0.5$, $c_0 = 0.07$, $c_1 = 0.5$, $d = -0.1$, $\epsilon = 1$ and $\mathbf{y}^F = (0.01, 1, 0.01)$; timeseries for three components of x and y_2 are shown. Successive epochs where the trajectory is close to the saddle equilibrium $\mathbf{q}_1$ and the chaotic saddles $\mathcal{A}_2$, $\mathcal{A}_3$ are labelled at the top of diagram. The connection $\mathbf{q}_1 \to \mathcal{A}_2$ is phase resetting as it follows a one-dimensional unstable manifold for the equilibrium $\mathbf{q}_1$.

these switch between the fixed point at $\mathbf{q}_1$ and the chaotic behaviour of $\mathcal{A}_j$ for $j = 2, 3$. On increasing c by a small amount we lose attraction of the cycle at a resonance and for this system, with $d < 0$, we appear to create an approximately periodic chaotic attractor – see the example illustrated in Figure 7 with $c_0 = 0.09$.

Examining the geometric rate of increase R as approximated by $R = T_{n+1}/T_n$ can clarify the behaviour for parameters on either side of the resonance bifurcation. Figure 8 shows this ratio plotted against the number of circumnavigations of the cycle for two different parameter values on either side of the resonance. In both plots, the solid line corresponds to

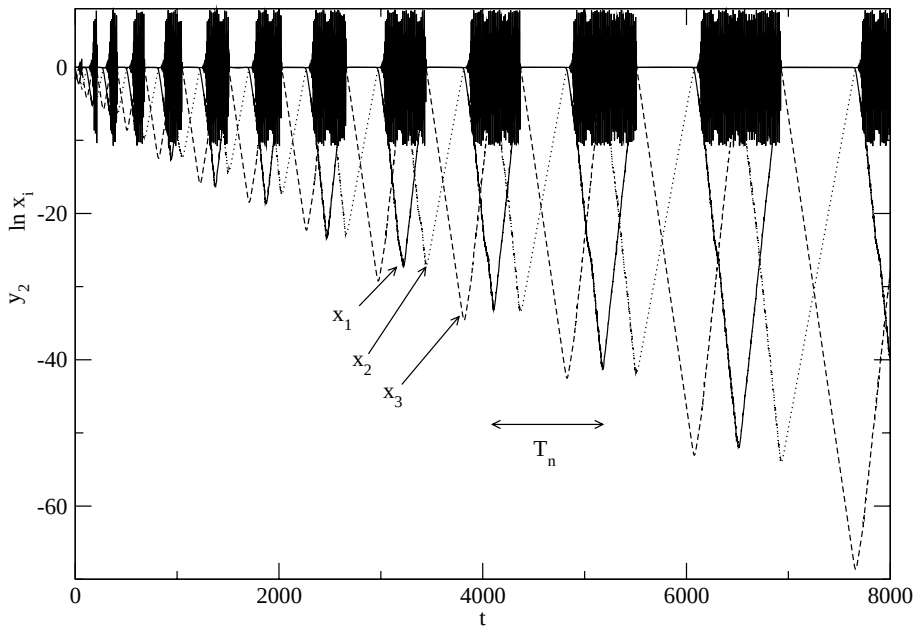

FIGURE 5. Attracting cycling chaos shown for same trajectory as Figure 4 but instead showing the logarithms of the x_i. The lengths of the phases T_n increase approximately geometrically as the trajectory approaches the cycle.

$\mathbf{y}^F = (0.01, -0.04, 0.04)$ and the dotted line to $\mathbf{y}^F = \mathbf{y}^A \approx (0.007, -0.035, 0.035)$ to within double precision accuracy. In plot (a) we have $c_0 = 0.08 > c_0^*$. We observe that T_{n+1}/T_n tends to unity on a periodic orbit for $\mathbf{y}^F \neq \mathbf{y}^A$. In contrast, for $\mathbf{y}^F = \mathbf{y}^A$ (dotted line) we find instead fluctuations about unity. Here R has a mean of 1.008 with a standard deviation of ± 0.0332. In (b), which has $c_0 = 0.072 < c_0^*$ we expect to find (for both values of $\mathbf{y}^F$) the ratio R tending to a value greater than one, which gives the exponent of the geometric rate of slowing. Both models clearly have T_{n+1}/T_n consistently greater than one, but neither has converged after 80 times around the cycle (the phase resetting system has $R = 1.024 \pm 0.0258$, and the non-phase resetting version has $R = 1.040 \pm 0.0327$). This is symptomatic of the difficulty of numerics for cycles – here the rate of convergence is very slow. We can increase this rate of convergence (and increase R) simply by decreasing c_0, but this also has the effect of making the dynamics approach E_{ij} much more quickly, and so fewer circuits round the cycle are possible before the calculations lose significance.

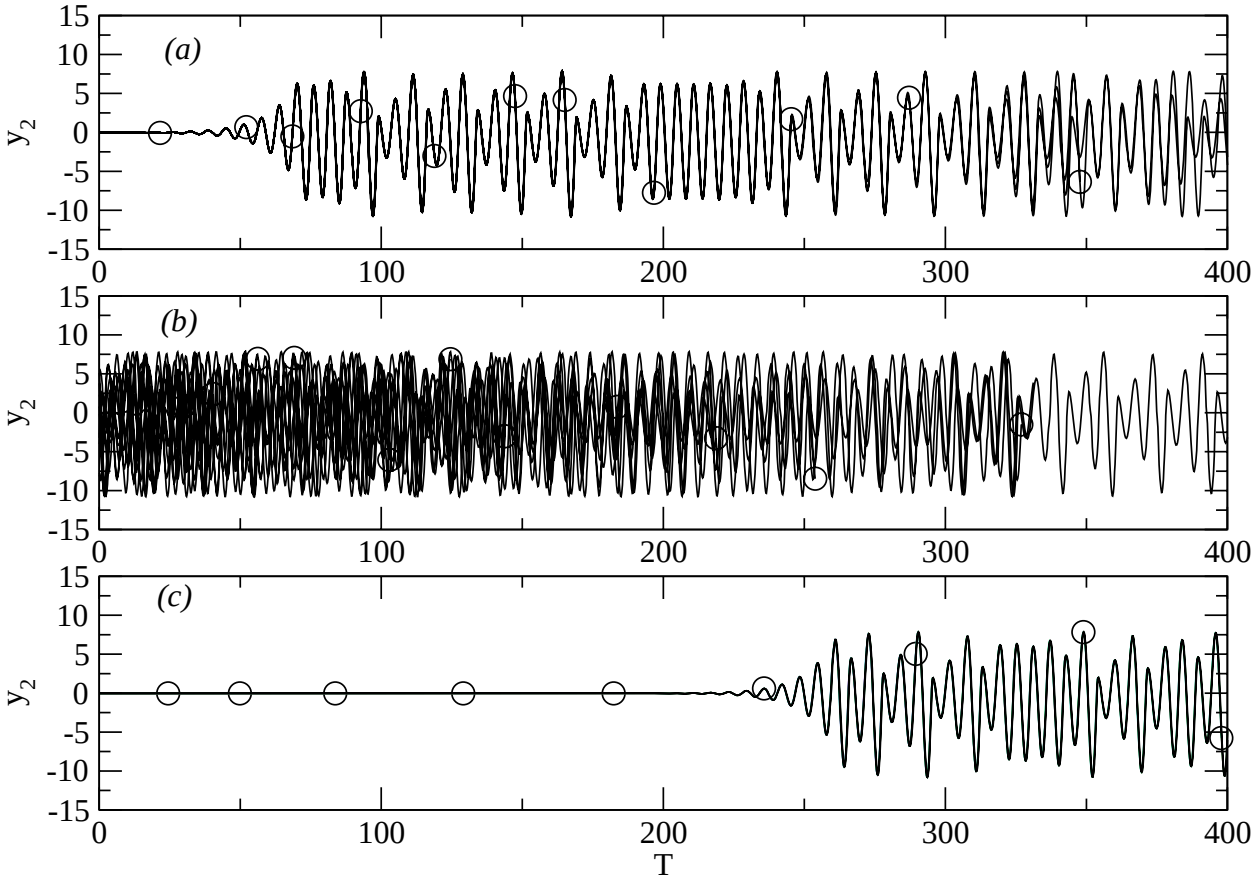

FIGURE 6. A number of orbit segments (of increasing length) are shown for (a) a phase resetting connection for the attractor of the trajectory in Figure 4. Each time the trajectory enters $|x_2| > 0.8$ we set T to 0 and each time it leaves $|x_2| > 0.8$ we mark by a circle. (b) This shows the non phase resetting connection between the chaotic saddles $\mathcal{A}_2$ and $\mathcal{A}_3$ for the same cycle. On entering $|x_3| > 0.8$ we set T to 0 and mark with a circle when we leave $|x_3| > 0.8$. The segments get longer each time around the cycle as the trajectory slows down, finally leaving a single signal for $T > 330$. Observe that there is no apparent coherence comparable to (a). (c) This shows a connection for the case as above but with $c_0 = 0.07$ and $\mathbf{y}^F = \mathbf{y}^A$ to double precision accuracy, with $T = 0$ on entering $|x_2| > 0.8$. Observe that after about 300 time units, numerical inaccuracies in specifying $\mathbf{y}^F$ cause the connection to head towards $\mathcal{A}_2$ as a phase resetting connection.

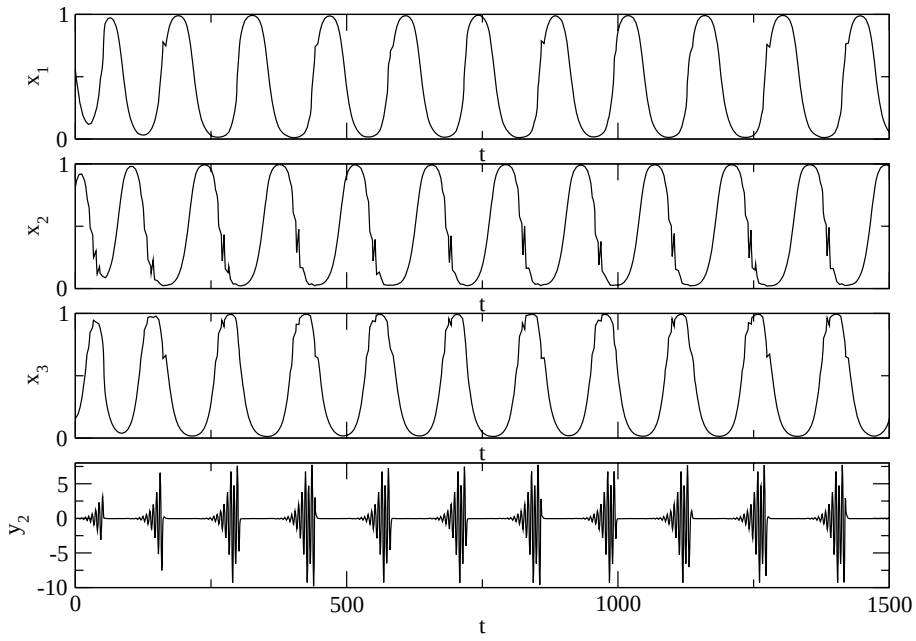

FIGURE 7. A trajectory approaching an approximately periodic chaotic attractor for the same parameters as Figures 4 and 5, but with $c_0 = 0.09$; timeseries for three components of x and y_2 are shown. The orbit includes segments of the one-dimensional unstable manifold for the equilibrium $\mathbf{q}_1$.

3.2. **Aspects of numerical simulation.** The numerical simulation of approach of trajectories to a cycling attractor, and in particular the selection of connection, is difficult to realize accurately because:

(1) There are directions with positive Lyapunov exponents within the chaotic saddles $\mathcal{A}_{2,3}$.
(2) The connection selected depends critically on the time of residence near a saddle, and this can become unbounded.

This means that we can only believe the qualitative behaviour of connection selection for residence times near saddles that are up to length T such that

$$\eta \exp(\lambda T) \ll 1$$

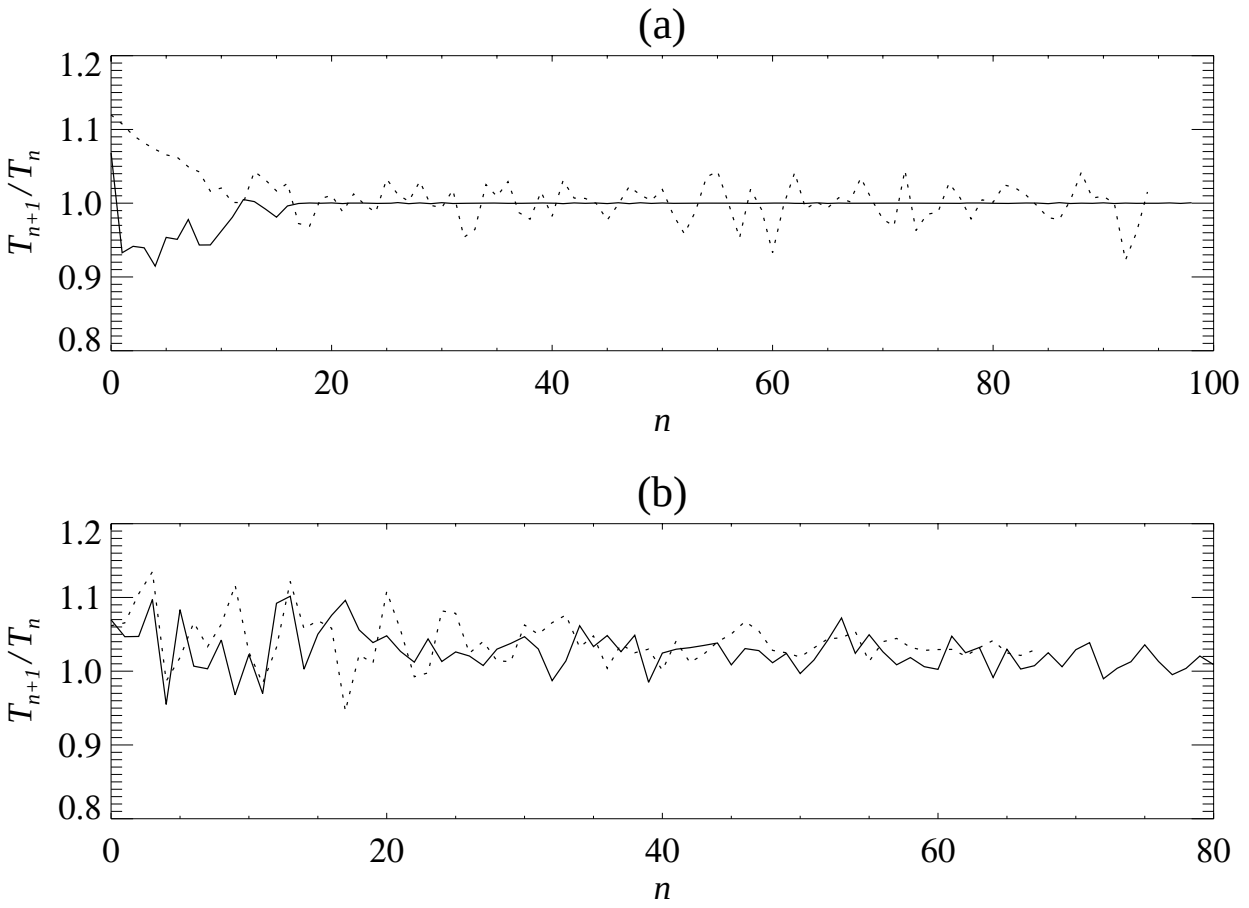

FIGURE 8. The ratio R of successive times T_n plotted against circumnavigations n. The fixed parameters are (as before) $b_0 = -0.1$, $b_1 - 0.5$, $c_1 = 0.5$, $d = -0.1$, $\epsilon = 1$. Solid lines represent the phase resetting model with $\mathbf{y}^F = (0.01, -0.04, 0.04)$ and dotted lines the non-phase resetting version with $\mathbf{y}^F = \mathbf{y}^A$ (to double precision accuracy). The control parameter values are (a) $c_0 = 0.08 > c_0^*$, (b) $c_0 = 0.072 < c_0^*$.

where λ is the most positive tangential Lyapunov exponent for the chaotic saddle and η is the machine accuracy. This means that we have an effective time-horizon

$$T < -\frac{\log(\eta)}{\lambda}$$

beyond which errors will have accumulated to the extent that different selection behaviour may appear. For the numerics in Section 3 we can estimate λ as approximately 0.0713 for the Rössler system. Hence for order one $\mathbf{y}$ at double-precision accuracy, we have $\eta = 10^{-16}$

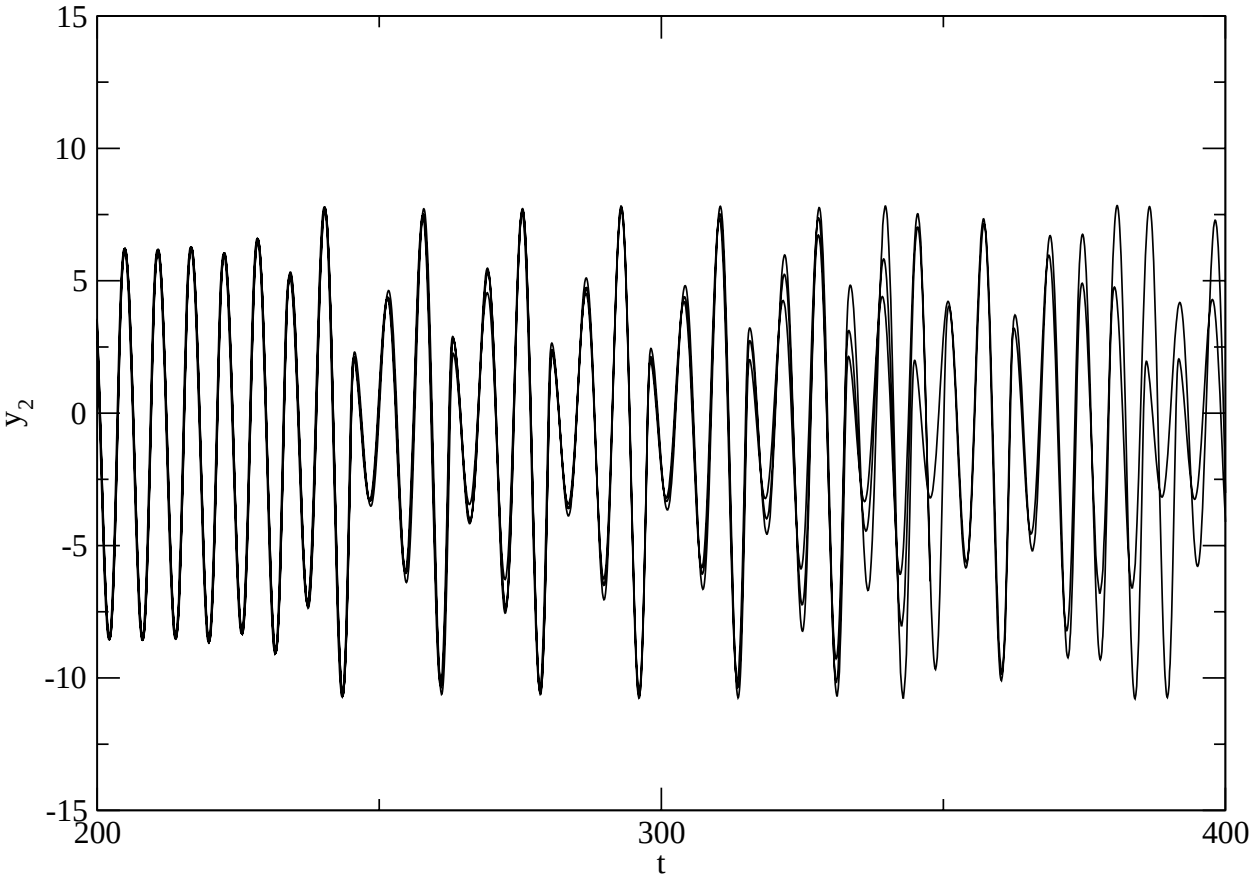

FIGURE 9. Loss of coherence after a phase resetting connection during attracting cycling. After approximately 300 time units for the trajectory segments shown in Figure 6(a) one loses coherence due to numerical inaccuracy.

and can expect separation from a phase resetting connection after a few hundred time units. Figure 9 illustrates this effect.

Even for cycles that are shorter than this, computation of Lyapunov exponents has to be done very carefully due to the fact that the local behaviour changes greatly as one moves around the cycle. Therefore, any Lyapunov exponent calculation will typically show very large fluctuations and slow convergence as the trajectory proceeds around the cycle.

A similar effect in the computation of approaches to invariant subspaces is observed in [7, 19] which can be overcome by representing the distance from the invariant subspace using an exponential numerical grid. This approach is not easily transferable to the sort of problem

we consider here, as the distance from a given trajectory $W^u(\mathbf{q}_1)$ (rather than from a single point) would need to be stored in an exponential grid.

Finally, we remark that we can change the choice of the numerical value 4 in the definition of the function μ so as to vary $\max \mu'$. However, that if $\max \mu'$ becomes too large, this can cause problems for the numerical integration. On the other hand, if $\max \mu'$ is too small then the coupling can create new invariant sets near those we are interested in and further complicate the dynamics.

4. Connection selection for non-phase resetting cycles

The attractors we observe in the model (1) are comprised of a finite number of *nodes* – saddle equilibria or chaotic saddles – together with possibly infinitely many *connections*.

In what follows, we continue to work within the fundamental domain $\mathbf{F}$. Let ϕ_t denote the flow of (1) restricted to $\mathbf{F}$. For $z \in \mathbf{F}$, $X \subset \mathbf{F}$, let $d(z, X) = \inf\{\|z - a\| \mid a \in X\}$ (and so if X is compact $d(z, X) = 0$ if and only if $z \in X$). If we define $\mathcal{A}_1 = \mathbf{q}_1$, then $\mathcal{A}_i \subset P_i$ is an attractor for the dynamics restricted to P_i, $i = 1, 2, 3$. The $\mathcal{A}_i$ are connected via the sets of connections

$$C_i = \{x \mid d(\phi_t(x), \mathcal{A}_{i+1}) \to 0 \text{ and } d(\phi_{-t}(x), \mathcal{A}_i) \to 0 \text{ as } t \to \infty\}.$$

Equivalently, we may write

$$C_i = W^u(\mathcal{A}_i) \cap W^s(\mathcal{A}_{i+1})$$

where $W^{u,(s)}$ are the unstable (resp. stable) sets of $\mathcal{A}_i$.

Provided that $\mathbf{y}^F \neq \mathbf{y}^A$, the cycle for (1) is given by

$$\Sigma = \bigcup_{i=1}^{3} \mathcal{A}_i \cup C_i.$$

We can define a connection C_i as being *phase resetting* if it is a single trajectory. In the case that C_i is not phase resetting, the following question arises.

Selection of connections: Given an asymptotically stable robust cycle Σ with basin of attraction $B(\Sigma)$, what is the *likely limit set* of $B(\Sigma)$ (in the sense of Milnor [18])? In other words, if we discount sets of zero measure in the basin of $B(\Sigma)$, what subset Σ' of Σ is unavoidable for the ω-limit sets of points in $B(\Sigma)$?

This problem was raised and partially addressed in [2] for a heteroclinic cycle between equilibria. It was found that for the two-dimensional connection sets studied that if E_i was the strongly unstable eigenspace at A_i then

- Σ' was typically a union of one-dimensional connections (corresponding to the strong unstable manifolds) if $\dim(E_i) = 1$.
- $\Sigma' = \Sigma$ if $\dim(E_i) = 2$, and the strongly unstable eigenvalues are complex.

Even for direct products of rather simple systems, the problem of cycle selection seems to be very subtle – see [4]. However, it is possible to obtain results showing an absence of cycle selection if we assume strong enough results on nodal dynamics (existence of Markov partitions). We refer to [4] for more details.

In the context of connections between chaotic sets, there is a new significant feature. Connections selected in an attractor determine the approach to the chaotic saddles and may for example select 'atypical' routes of approach that give different Lyapunov exponents to that expected for any 'natural' measure.

For model (1) in cases where the C_i are more than one dimensional, we do not understand which connections will typically be selected, and this may be a feature that is vital in understanding the dynamics near more general chaotic itinerant attractors. As we see in the final section, even numerical simulations are not at all easy to interpret. Possibly, a better approach is to consider a noise-perturbed system in which case cycle selection will only occur on a probabilistic level.

5. Discussion

In summary, we have introduced a new model system in which one can observe a variety of cycling attractors with and without phase resetting. The effect of phase resetting is not possible in the system discussed in [1] because it is a global skew product. This model system is locally well-approximated by a skew product near each of the nodes, but is not globally a skew product. Although the system is carefully constructed to have the desired behaviour, it should be stressed that the connections will be robust to any perturbation of the system as long as the symmetries are preserved and the nature of the chaos is not changed too greatly. In this sense, the values of the parameters and the exact forms of the functions chosen are relatively unimportant.

We believe that the property of phase resetting deserves closer examination in more general chaotic itinerant attractors, as does the question of cycle selection which may be helpful in a better statistical understanding of these attractors.

References

[1] P. Ashwin, Cycles homoclinic to chaotic sets; robustness and resonance. *Chaos* **7** 207–220 (1997).

[2] P. Ashwin and P. Chossat. Attractors for robust heteroclinic sets with a continuum of connections, *J. Nonlinear Sci.* **8** 103–129 (1997).

[3] P. Ashwin and M. Field. Heteroclinic networks in coupled cell systems. *Arch. Rational Mech. Anal.* **148** 107–143 (1999).

[4] P. Ashwin and M. Field. *Product dynamics for heteroclinic attractors.* In preparation (2003).

[5] P. Ashwin, A.M. Rucklidge and R. Sturman. Infinities of periodic orbits near robust cycling, *Phys. Rev. E* **66** 035201(R) (2002).

[6] P. Ashwin, A.M. Rucklidge and R. Sturman. *Cycling attractors of coupled cell systems and dynamics with symmetry* Submitted to proceedings of NATO ASI on Synchronization, Crimea, May 2002.

[7] P. Ashwin and A.M. Rucklidge. Cycling chaos: its creation, persistence and loss of stability in a model of nonlinear magnetoconvection. Physica D **122** 134–154 (1998).

[8] T. Chawanya, Coexistence of infinitely many attractors in a simple flow. *Physica D* **109** 201–241 (1997).

[9] S.-N. Chow, B. Deng and B. Fiedler, Homoclinic bifurcation at resonant eigenvalues. *J. Dyn. Diff. Eqns.* **2** 177–244 (1990).

[10] M. Dellnitz, M. Field, M. Golubitsky, A. Hohmann and J. Ma, Cycling chaos. *I.E.E.E. Transactions on Circuits and Systems: I. Fundamental Theory and Applications*, **42** 821–823 (1995).

[11] M Field, *Dynamics, Bifurcation and Symmetry*, Pitman Research Notes in Mathematics, **356**, 1996.

[12] W.J. Freeman and C.A. Skarda, Spatial EEG patterns, nonlinear dynamics and perception – the neo-sherringtonian view. *Brain Research Reviews* **10** 147–175 (1985).

[13] J. Guckenheimer and P. Holmes, Structurally stable heteroclinic cycles, *Math. Proc. Camb. Phil. Soc.* **103** 189–192, (1988).

[14] D. Hansel, G. Mato and C. Meunier, Clustering and slow switching in globally coupled phase oscillators. *Phys. Rev. E* **48** 3470–3477 (1993).

[15] H. Kori and Y Kuramoto, Slow switching in globally coupled oscillators: robustness and occurrence through delayed coupling. *Phys. Rev. E* **63** 046214 (2001).

[16] K. Kaneko. On the strength of attractors in a high-dimensional system: Milnor attractor network, robust global attraction, and noise-induced selection. *Physica D* **124** 308–330 (1998).

[17] M. Krupa, Robust heteroclinic cycles. *Journal of Nonlinear Science* **7** 129–176 (1997).

[18] J. Milnor. On the concept of attractor. *Commun. Math. Phys.* **99** 177–195 (1985); Comments *Commun. Math. Phys.* **102** 517–519 (1985).

[19] A. Pikovsky, O. Popovych and Yu. Maistrenko, Resolving clusters in chaotic ensembles. *Phys. Rev. Lett.*, **87** 044102 (2001).

[20] O.E. Rössler Continuous chaos: four prototype equations, *Bifurcation theory and applications*, Eds O. Gurel and O.E. Rössler, *Ann. N. Y. Acad. Sci.* **316**:376–392 (1979).

[21] M. Timme, F. Wolf, and T. Geisel. Prevalence of unstable attractors in networks of pulse-coupled oscillators. *Phys. Rev. Lett.* **89** 154105, (2002).

School of Mathematical Sciences, University of Exeter, Exeter EX4 4QE, UK
E-mail address: P.Ashwin@ex.ac.uk

Department of Mathematics, University of Houston, Houston, TX 77204-3008, USA
E-mail address: mf@uh.edu

Department of Applied Mathematics, University of Leeds, Leeds LS2 9JT, UK
E-mail address: A.M.Rucklidge@leeds.ac.uk

Department of Applied Mathematics, University of Leeds, Leeds LS2 9JT, UK
E-mail address: rsturman@amsta.leeds.ac.uk